CrossMark

ORIGINAL PAPER

Fabrication of gold nanoparticle-coated paper and its use as a sensitive substrate for quantitative SERS analysis

Javier E. L. Villa[1] · **Diego P. dos Santos**[1] · **Ronei J. Poppi**[1]

Abstract This paper describes a rapid method for fabrication of a paper substrate coated with gold nanoparticles (GNPs) that results in the formation of a large number of hot spots on the surface and allows an adequate control of the active area. The resulting substrate is shown to be a viable material for use in quantitative surface-enhanced Raman spectroscopy (SERS) analysis. The influence of the amount of GNPs on the SERS signals (using crystal violet as a sample analyte) was correlated with field-emission scanning electron microscopy, UV-visible and theoretical studies. The use of this substrates results in larger enhancement of Raman signals and in comparably repeatability when compared to commercially available substrates. The substrate was applied to SERS-based determination of nicotine and uric acid in aqueous solution, and the respective limits of detection are 20 and 30 $\mu g\ L^{-1}$. The results indicate that the SERS substrates may be applied to the quantification of a wide variety of molecules.

Keywords Surface-enhanced Raman spectroscopy ·
FE-SEM · Mie theory · Crystal violet · Nicotine · Uric acid

Introduction

Surface-enhanced Raman spectroscopy (SERS) is a powerful technique that increases the Raman scattering efficiency, by a combination of electromagnetic and chemical contributions, when the target molecule is adsorbed on plasmonic metallic nanostructures (SERS substrates), typically made of gold or silver [1]. Since its discovery, SERS has gained considerable attention due to its several advantages and investigation possibilities in sensitive analysis, even at the single-molecule level [2]. Thus, the applications of SERS in analytical chemistry include the trace detection of pathogens [3], biomolecules [4], pesticides [5], food contaminants [6] and drugs [7]. Furthermore, in recent years, many advances in SERS were related to the fabrication of novel substrates with different architectures, considering that the geometry, size and homogeneity of the SERS substrates are key parameters which determine their efficiency (in terms of sensitivity and repeatability), and consequently their applicability for quantitative analysis [8].

Nanoparticles in colloidal aqueous solutions have been usually employed as SERS substrates; however, their applications are challenged by the poor stability, low repeatability, and the difficulty for working in non-aqueous media. Currently, typical methods to fabricate efficient SERS substrates include the immobilization of metallic nanoparticles on rigid substrates (glass, quartz and silicon) [9, 10], or the fabrication of metallic nanostructures by template techniques [11], focused ion beam patterning [12] and lithography [13]. Nevertheless, these methods are time-consuming and/or require sophisticated equipment (high cost-demanding). On the other hand, flexible substrates such as paper, polymers, carbon nanotubes and graphene have shown potential to replace the rigid substrates, in view of their low-cost, facile processability and eco-friendly properties [14]. Paper, in particular, has been successfully utilized as a biodegradable substrate in microfluidic systems [15], diagnostic devices [16], and, recently, in SERS [17].

The most common methods for preparation of metal nanoparticle-paper substrates are the mirror reaction [18, 19]

✉ Ronei J. Poppi
ronei@iqm.unicamp.br

[1] Institute of Chemistry, University of Campinas, P. O. Box 6154, Campinas, SP 13081-970, Brazil

Springer

(for silver nanoparticles) and dip-coating [17, 20] (for gold or silver nanoparticles). Moreover, gold is preferred instead of silver, when using near-infrared excitation, due to its higher chemical stability and facile synthesis [1]. The dip-coating method consists in the immersion of paper into a fixed volume of gold nanoparticles solution, followed by drying. It results in flexible SERS substrates with homogenous distribution of the gold nanoparticles on the paper surface [17].

Although dip-coating method has gained significant interest due to its simplicity, the need of long preparation time (at least 12 h) and the relatively large amount of gold nanoparticles used per substrate (10 mL of colloidal gold nanoparticles) [17, 21] limit the large-scale fabrication of paper-based SERS substrates. Furthermore, there are few studies about the control of the deposition of gold nanoparticles within paper, and none has optimized the hot spots generation on the paper surface. Therefore, the designing and assembling of paper-based substrates for SERS applications still requires further improvement.

To be considered an efficient alternative to the commercial SERS substrates, the paper-based substrates should be sensitive, reproducible, easily produced on large-scale and capable to be used in the quantification of a wide variety of molecules. To achieve this goal, the primary objectives of this work are (i) to develop a rapid and efficient strategy to prepare paper-based SERS substrates, (ii) to study the effect of the amount of gold nanoparticles on the SERS signals of crystal violet, (iii) to compare the sensitive and the reproducibility of the gold nanoparticle-paper hybrid with commercially available substrates, and (iv) to quantify nicotine (an addictive drug present in tobacco and several pharmaceutical products) and uric acid (a disease biomarker) in aqueous media using the paper-based SERS substrates.

Experimental

Instrumentation

All SERS measurements were performed using a dispersive spectrometer Raman Station 400 F (PerkinElmer, MA, USA), equipped with a camera image and a 785 nm near-infrared diode laser operating at 100 mW (at source). The spectra were acquired after 5 exposures of 5 s each.

The characterization of colloidal gold nanoparticles and gold nanoparticle-paper hybrid were performed by UV-vis spectroscopy (Cary probe 5000 UV-vis) and field emission-scanning electron microscopy (FE-SEM, Quanta FEG 250). Gold films (100 nm) were deposited onto paper and onto alumina via sputtering (Oerlikon Balzers BA510, Schaumburg, IL), and were used to compare their optical properties with those of paper-based SERS substrates.

Chemicals

Milli-Q1 Ultrapure Water Purification System (Millipore, Brussels, Belgium) provided the deionized water used to prepare all standards and solutions. Tetrachloroauric acid (HAuCl$_4$, 30 % m/m), anhydrous sodium citrate, and uric acid were purchased from Sigma-Aldrich. Crystal violet and nicotine (>99 %) were obtained from Fluka. Laser printer paper (75 g m^{-2}) was purchased from Chamex (Sao Paulo, SP, Brazil) and was used to prepare all the paper-based SERS substrates.

Synthesis of gold nanoparticles

The synthesis of gold nanoparticles (GNPs) was made based on Turkevich method [22]. Briefly, an aliquot of 40 µL of tetrachloroauric acid (30 %, m/m) was mixed with approximately 100 mL of water and heated until the boiling point (approx. 100 °C), then 1.4 mL of anhydrous sodium citrate solution (2 %, m/v) was added into the mixture under magnetic stirring for 5 min. Finally, stirring was interrupted and GNPs solution was cooling at room temperature.

Preparation of paper-based SERS substrates

Figure 1 shows the system for rapid preparation of flexible SERS substrates. It consists in two Teflon templates with six circular holes in one of them (4 mm of diameter), that allows the control of the substrate active area. Aliquots of 20 µL of GNPs were added in four concentration levels: 3-fold dilution, without preconcentration, 10-fold and 50-fold preconcentration. To obtain the preconcentred GNPs, the
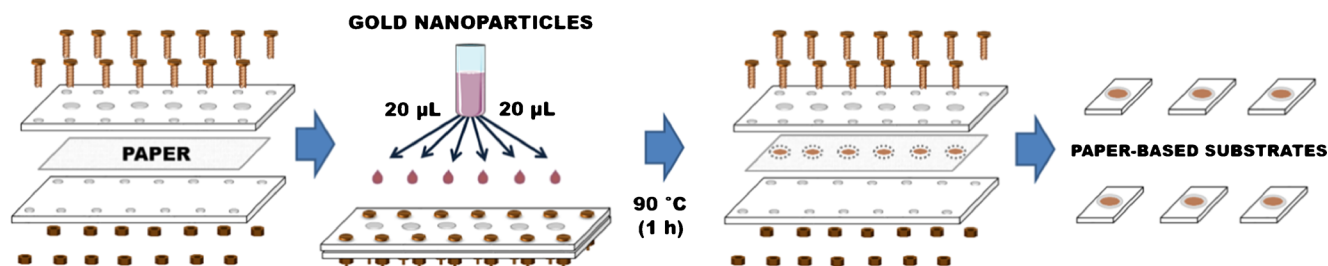
Fig. 1 Procedure for rapid preparation of paper-based SERS substrates

colloid was centrifuged for 15 min at 1600 x g and an adequate volume of supernatant was discarded. After GNPs addition, the system was placed into oven at 90 °C by 60 min and then placed on pieces of glasses of 1 cm × 1 cm for facile handling.

To obtain the analyte SERS spectra (crystal violet, uric acid or nicotine), the prepared SERS substrates were individually immersed for 20 min in the analyte solution and drying under dry-air stream. The SERS spectra were then collected at five different points of the substrate active area and the experiments were performed in triplicate ($n = 15$). Crystal violet was used as molecule probe to evaluate the best conditions for fabricating paper-based substrates. Under these optimized conditions, the prepared SERS substrates were employed to perform the quantitative detection of uric acid and nicotine in aqueous solution. The limit of detection and limit of quantification were calculated as three and ten times the standard deviation of the blank signal, respectively.

Commercial SERS substrates

Klarite® substrates were purchased from Renishaw diagnostics Ltd. (Glasgow, U.K.). These substrates present a highly regular nanostructured gold surface formed by inverted squared pyramids and an active area of 4 mm × 4 mm [23]. To acquire the SERS spectra, 0.5 μL of crystal violet 2 mg L^{-1} was pipetted onto the SERS active area after which the solvent was left to evaporate at room temperature by approximately 30 min. The SERS spectra were then collected at five different points and the experiments were carried out in triplicate ($n = 15$).

Classical electrodynamics simulations

In order to better understand the experimental results (SERS signal intensifications for different GNP concentrations), numerical simulations based on the generalized Mie theory [24, 25] were performed for different arrays of GNPs. In all simulations, the optical response of gold was described by the experimental values for the dielectric function from Johnson and Chisty compilation [26].

Results and discussion

Preparation of GNP-coated paper

The synthesis of colloidal GNPs resulted in a red-wine colored suspension with citrate groups acting as reducing agent and stabilizer, providing the negative charge on GNPs surface (colloidal stability) [27]. The analysis by UV-vis spectroscopy showed the characteristic optical signature of spherical GNPs in solution, with a surface plasmon band at 532 nm. The characterization by FE-SEM microscopy allowed the calculation of the mean diameter (45 ± 6 nm, $N = 100$) of homogeneous GNPs (Fig. S1). Also, considering the near-infrared excitation source employed (785 nm), the use of gold nanoparticles for fabricating SERS substrates can provide a similar signal intensification and a higher chemical stability in comparison to the use of silver nanoparticles [1].

The GNPs were deposited on paper using an efficient strategy, as showed in Fig. 1. Although this system allows the control of surface active area by using the circular holes in the Teflon template (on the top), the use of filter paper is not adequate in this case due to the capability of GNPs to migrate through the bulk [17]. To overcome this difficult, printer paper was used due to its greater number of fibers per area, therefore minimizing the migration of GNPs among the fibers and providing a better control of both, the SERS active area and the amount of GNPs deposited per substrate. The procedure employs small volumes of colloidal GNPs (20 μL) in combination with a drying step at 90 °C, that resulted in the reduction of preparation time when compared with dip-coating method (see Table 1). Therefore, this method integrates the rapidity, easy handling and large-scale advantages in the production of paper-based SERS substrates without residues generation (green method).

Optimizing the GNP concentration

Taking advantage of the use of small volumes of colloidal GNPs, it is possible to use very high or very low concentration levels of GNPs during the fabrication of SERS substrates without the need to extend the time of preparation or to employ a large amount of GNPs. Thus, the influence of the

Table 1 Comparison of procedures for preparation of metal nanoparticle-paper hybrid

Metal	Procedure / Preparation time	Limitation	Reference
Gold	Direct deposition / 1 h	Preconcentration is required	This work
Gold	Dip-coating / 24 h	Long preparation time	[17]
Gold	Dip-coating / 12 h	Long preparation time	[21]
Silver	Mirror reaction / few minutes	Lower chemical stability[a]	[18]
Silver	Mirror reaction / few minutes	Lower chemical stability[a]	[19]
Silver	Dip-coating / 24 h	Lower chemical stability[a] and long preparation time	[20]

[a] In comparison to gold nanoparticle-paper hybrid

amount of GNPs on the SERS signal of crystal violet and on the background signal was studied, and the results are presented in Fig. 2.

Figure 2a shows the SERS spectra of crystal violet 2 mg L^{-1}, obtained using the paper-based substrates prepared with different GNPs concentrations. The SERS spectra presented intense characteristic peaks at 418 cm^{-1} (phenyl-C-phenyl and C-N bending), 1174 cm^{-1} (C-phenyl and C-H stretching), 1373 cm^{-1} (C-N and phenyl-C-phenyl stretching), 1614 and 1582 cm^{-1} (C-phenyl stretching) [28, 29]. Moreover, the intensity for all of these peaks increased with the amount of GNPs deposited up to 10-fold preconcentration, after which a decrease in SERS intensities for an excess of deposited GNPs (50-fold preconcentration level) was observed. On the other hand, the Fig. 2b shows that the background signals of the prepared SERS substrates present some peaks, probably arising from the printer paper components (cellulose, coating and polymers). The results also showed that the intensity of the background signal was dramatically reduced when higher amounts of GNPs were employed to prepare SERS substrates. Therefore, taking into account these results (SERS and background signals), a 10-fold preconcentration level prior to GNPs deposition was identified as the best condition to prepare highly sensitive paper-based SERS substrates. Additionally, it is important to note that although the procedure requires a preconcentration step, the volume of GNPs used per substrate in the optimized conditions (20 μL of 10-fold preconcentrated or 0.2 mL of colloidal GNPs) is much smaller than that commonly used in the dip-coating method (10 mL of colloidal GNPs).

## Interpretation of the GNP concentration effect and theoretical support

The distribution of GNPs on the paper surface for all the concentration levels was studied by FE-SEM (Fig. 3). The microscopies showed that GNPs were dispersed and adsorbed on paper surface forming hot spots, suggesting that even though paper has a weak negatively charged surface (hydroxyl cellulose groups), the GNPs can be retained on the paper surface by van der Waals interaction [30]. Furthermore, as showed in Fig. 3d, a 50-fold preconcentration of GNPs prior to deposition can promote large agglomeration of GNPs and the formation of multiple layers.

The lower SERS intensities observed when using diluted and non-preconcentred GNPs (Fig. 2a) can be explained by the lower surface density of GNPs on the paper surface (Figs. 3a and b). This results in a lower density of hot spots, and also may be the reason for the observation of a larger background signal in the spectra (Fig. 2b) due to the larger paper area exposed to the laser excitation. For the preconcentrated GNPs, the exposed paper area is much smaller, hence decreasing the background signal (Fig. 2b). However, the observed SERS signal differences between the 10- and 50-fold preconcentration levels is not in agreement with the density of GNPs interpretation, according to which it is expected a larger SERS intensity for the 50-fold preconcentration level. This result suggests that besides the GNPs surface density, the electromagnetic coupling between the GNPs in the multilayer system is fundamental to the observed SERS intensities. To account for such contributions in the prepared substrates, UV-Vis spectra were obtained and are presented in Fig. 4. Figure 4a shows the variation of the optical properties when the amount of GNPs increases on the paper surface, whereas Fig. 4b shows the comparison among the optical responses for the substrate prepared with a 50-fold preconcentration level (which presented the largest difference in optical response) and two Au (100 nm thick) deposited films onto paper and alumina by the sputtering method.

The results of Fig. 4 show that the optical properties of the paper-based substrates with the increasing of GNPs concentration tend to be similar to that observed in gold (roughened) films, for which the surface plasmon resonance is a result of defects on the fabricated film. These results suggest that for the high GNPs concentrations, the surface plasmon resonances behave as extended modes, where the optical response for different wavelengths comes from defects on the GNPs
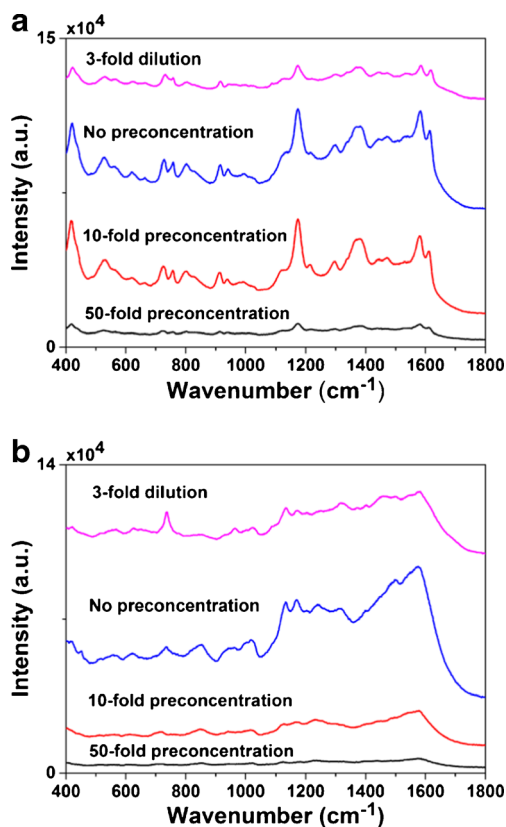
Fig. 2 **a** Average SERS spectra of crystal violet 2 mg L^{-1} and **b** average background signals of the paper-based substrates prepared using different concentration levels of GNPs (n = 15)
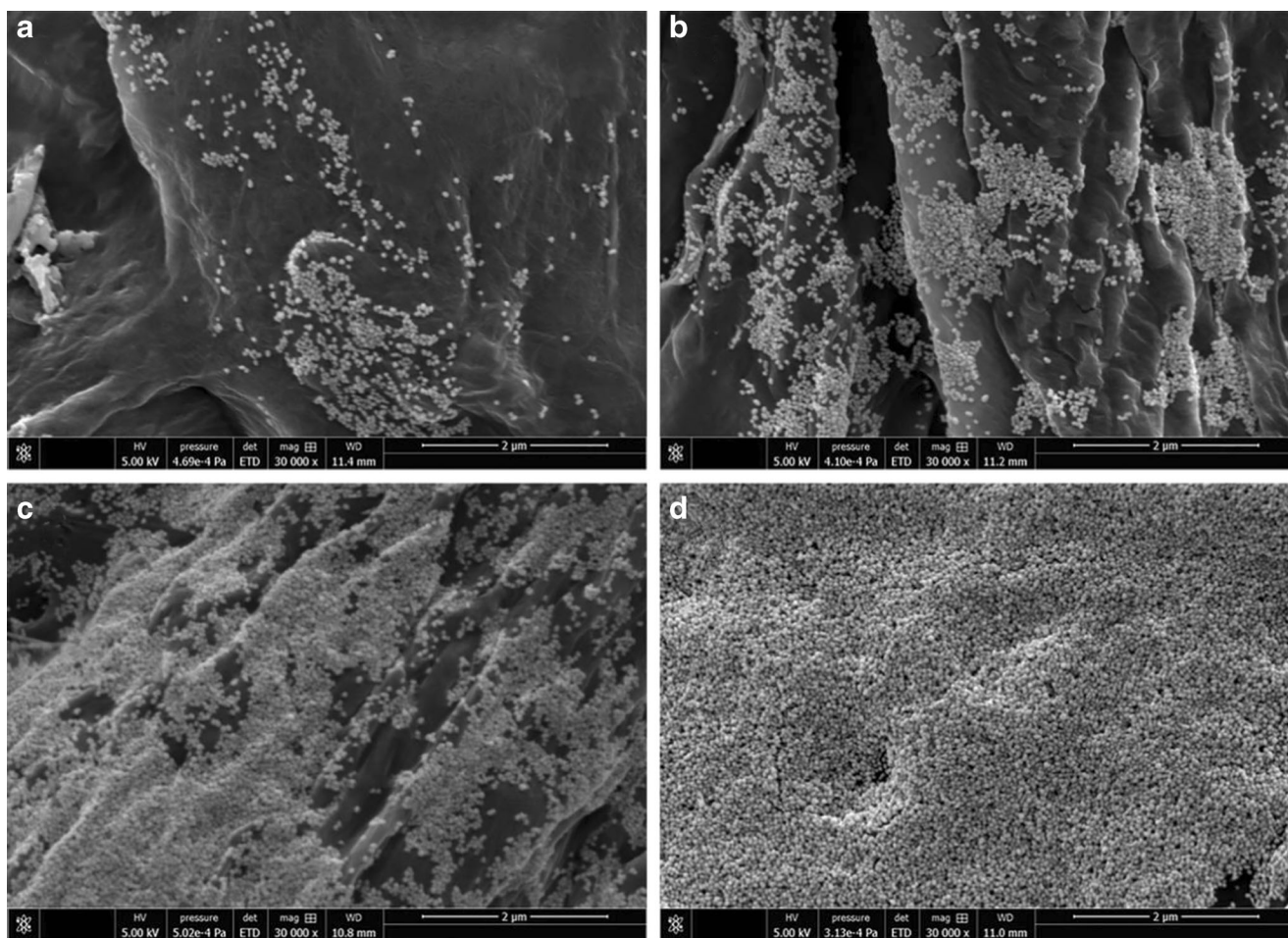
Fig. 3 FE-SEM studies for the paper-based substrates prepared with colloidal GNPs after **a** 3-fold dilution, **b** no preconcentration, **c** 10-fold preconcentration and **d** 50-fold preconcentration

film formation. An important characteristic of extended modes (coupling between multiple particles) is that the electric field concentration at the hot spots becomes smaller, in contrast to small particle clusters, for which the electric field enhancement in the vicinity between particles is extremely localized. To show such decrease in the field localization and its effects on the SERS intensity of molecules, GMT simulations were performed and the results for a simple model is presented in Fig. 5.

Figure 5a shows the simulated extinction spectra for a model system comprised of 1 (black solid line) and 2 (red solid line) hexagonal close packing layers (inset). The extinction spectra clearly show that the increasing amount of layers leads to the appearance of redshifted surface plasmon bands, due to coupling between the surface plasmon modes in each layer. In this figure it is also shown the incident laser wavelength in the SERS experiments ($\lambda_0 = 785$ nm, dashed vertical line). To account for the effect of the coupling between the two layers on the SERS intensities, the enhancement factor (EF, SERS intensity is proportional to EF) was calculated by using the magnitude of the electric field at an arbitrary point of the

nanoparticle surface (E_{loc}) and the magnitude of the incident electric field (E_0), as showed in Eq. 1 [31].

$$EF = \left[\frac{E_{loc}(785nm)}{E_0(785nm)} \right]^4 \qquad (1)$$

The observed SERS intensity in the above experiments, correspond to the average SERS intensities of molecules in different positions of the surface of each illuminated GNP. Therefore, a correct description of the SERS intensity tendency with the increase in the number of layers, should be given by the surface average EF for a given set of particles. To prevent time-consuming simulations, we present in Fig. 5b the surface average (<EF>) on the central particle for plane in black in the inset of Fig. 5a, which is below the plane in red. Therefore, we compare the surface average EF values for the same particle in both situations (1 and 2 layers). The insets of Fig. 5b shows the EF values on the surface of the central GNP in both situations, as described in the figure. It can be seen that in the 2-layer system, the highest EF values (red) spread over a large area (compared to the 1-layer system). However, it can
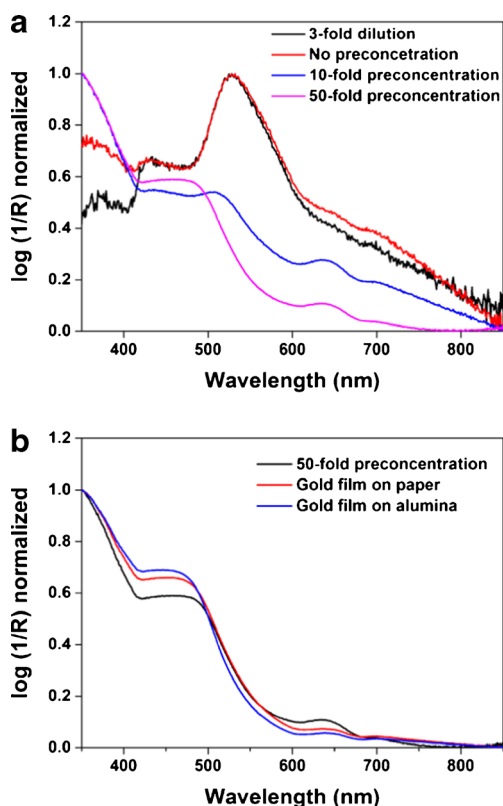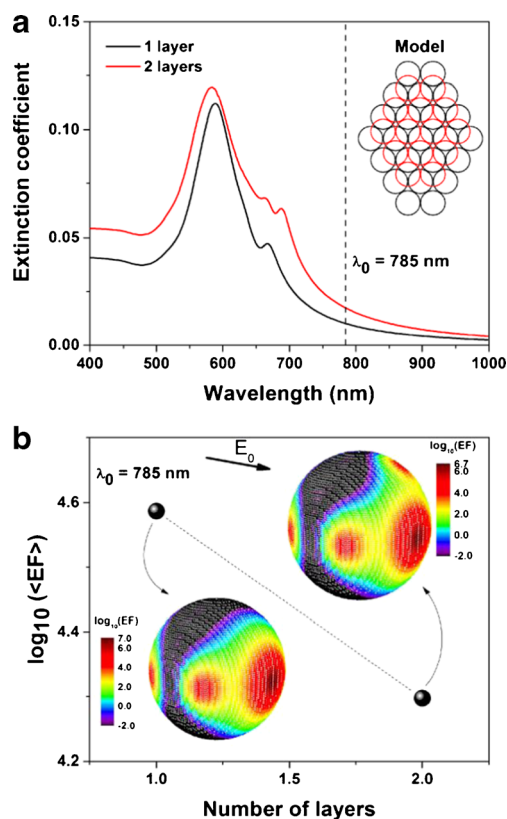
Fig. 4 UV-vis spectra of **a** paper-based substrates prepared using different GNPs concentrations and **b** gold films and paper-based substrate prepared after 50-fold preconcentration of GNPs

Fig. 5 a UV-vis spectra and **b** evaluation of the enhancement factor for different number of GNPs layers predicted by the theoretical model

be seeing that such increase in the EF area is accompanied by a decrease in the maximum EF value ($10^{6.7}$ and 10^7 for the 2 and 1 layers system, respectively), which is in accordance to our previous statement that the increase in the number of layers leads to a collective interaction that decreases the hot spots efficiencies in concentrating the local electric field. The SERS intensity is, therefore, a balance between these two factors: the spread in the EF values and increase in the hot spot efficiencies. The results for the surface average EF values are also presented in Fig. 5b. It shows a decrease in the EF values with the second layer by 26 %. This indicates that this simple model can explain the experimental results.

Gold nanoparticle-coated paper vs commercial SERS substrates

A commercial and highly reproducible SERS substrate (Klarite) was used to evaluate the performance of the paper-based SERS substrates (prepared in the optimized conditions). As can be observed in Fig. 6, the SERS spectrum of crystal violet 2 mg L^{-1} obtained by using the paper-based SERS substrates experienced a higher intensification than that observed using Klarite® substrates. This observation can be explained by the aleatory distribution of GNPs on the paper

fibers, generating a greater number of hot spots and then a higher intensification of local electric field.

Due to the large difference between the signal intensities, the relative standard deviation (RSD) was employed to compare the repeatability of both substrates. The RSD was calculated using the standard deviation (s) and the average signal (X), as showed in Eq. 2.

$$RSD = \left(\frac{s}{X}\right)x100\% \qquad (2)$$
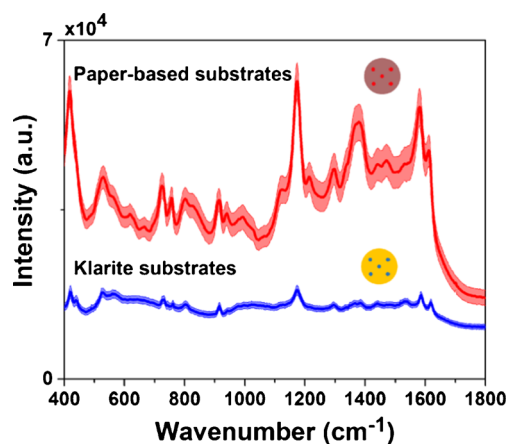
Fig. 6 Average and standard deviation of the SERS spectra of crystal violet 2 mg L^{-1} (collected in five different points and in triplicate, $n = 15$), obtained using paper-based substrates and Klarite substrates

The repeatability of both substrates was compared in a wide range of wavenumbers (400–1800 cm^{-1}), and similar RSD were observed: in the range of 5–10 % for paper-based substrates and 3–7 % for Klarite® substrates. This unexpected point of advantage arises from the fact that the laser covers an area with a great number of paper fibers instead of individual fibers (irregular surface). Additionally, although Klarite® substrates are highly regular nanostructures, the main source of variations in the SERS signal might arising from the non-homogeneous way in which the dropped sample is dried, also known as the "ring coffee effect" [32]. Thus, these results suggest that the paper-based SERS substrates are sensitive, reproducible and can be considered as an excellent alternative to the commercially available substrates.

Quantitative detection of nicotine and uric acid

The sensitive detection of dyes and sulfur-containing molecules have been extensively studied using a great variety of SERS substrates, probably because these type of molecules usually present great signal intensifications and can be easily adsorbed on metallic surfaces. However, a "good" SERS substrate should be also able to be used for the detection of a wide variety of molecules. Thus, in order to demonstrate the capability of the paper-based SERS substrates to be used in the quantification of relevant analytes, nicotine and uric acid were determined in aqueous media.

Nicotine is an addictive drug composed of pyridine and pyrrolidine groups, and can be found in tobacco and several pharmaceutical products. Fig. S2 shows the behavior of the most intense nicotine peak, localized at 1028 cm^{-1} (symmetrical breathing), with the variation of the nicotine concentration. The peak area was calculated at different nicotine concentrations in order to identify the linear working range (Fig. 7a). The peak area increased linearly with the concentration up to 1 mg L^{-1} and after that no significant increment in the response was observed. Thus, the linear working range for nicotine quantification was 0.06–1 mg L^{-1}, and the limits of detection and quantification were 0.02 and 0.06 mg L^{-1}, respectively.

Uric acid is an end product of nucleoside catabolism, and an important biomarker in urine and serum because high levels of uric acid in these fluids are associated to renal diseases and preeclampsia (a hypertensive disorder that occurs during pregnancy) [33]. The behavior of the uric acid SERS spectra at different concentrations was evaluated, as showed in Fig. S3. The increment of the intensity in the peaks at 492 cm^{-1} (C-N-C ring vibration) and at 638 cm^{-1} (skeletal ring deformation) was observed, and then the peak area of the most intense of them (638 cm^{-1}) was calculated at different concentrations, as can be seen in Fig. 7b. The limits of detection and quantification were 0.03 and 0.09 mg L^{-1}, respectively, and the linear range was ranged between 0.09 and 2 mg L^{-1}.
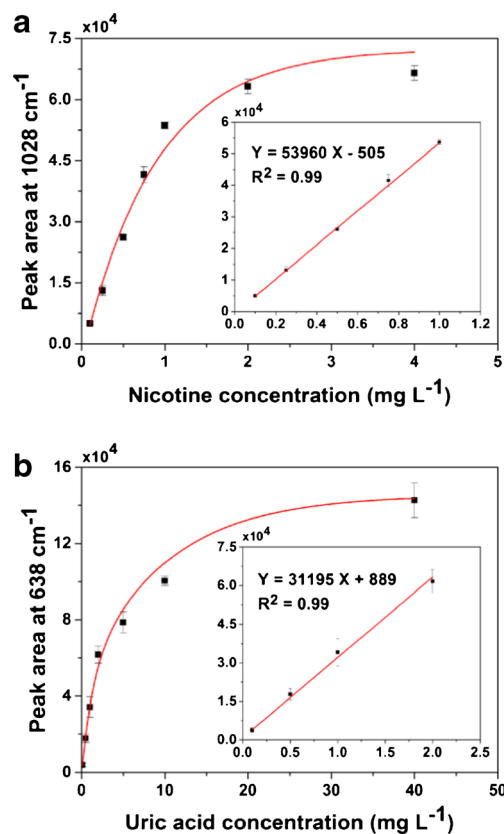
Fig. 7 Identification of the linear working range for the quantitative detection of **a** nicotine and **b** uric acid in aqueous media

The linear working ranges and the limits of detection found for nicotine and uric acid compare favorably with earlier results obtained by chromatography techniques [34, 35]. This shows these SERS substrates to be a viable material for the quantification of these analytes in real samples. However, the evaluation of interferences and the matrix effect should be assessed depending on the complexity of the sample to be analyzed.

Conclusions

In summary, we devised a rapid and efficient way to fabricate low-cost, sensitive and reproducible paper-based SERS substrates able to be used for quantifying a wide variety of molecules. The experimental results, corroborated by theoretical calculations, demonstrated that the amount of GNPs deposited on the paper fibers is a key parameter that determines the optimal SERS signal enhancement. Although a preconcentration step is required for its fabrication, the paper-based SERS substrates present several advantages such as a high sensitivity and a good repeatability, and their fabrication can be easily scaled to medium or large quantity production. Additionally, these substrates can be used to quantify nicotine and uric acid at clinically relevant concentration

levels, and can probably be used in a wide range of molecular systems.

Compliance with ethical standards

Conflict of interest The authors declare that there are no conflicts of interest.

References

1. Etchegoin PG, Ru ECL (2010) Basic electromagnetic theory of SERS. In: Schlücker S (ed) surface enhanced Raman spectroscopy: analitical, biophysical and life science applications. Weinheim, Germany, pp. 1–37

2. Kneipp J, Kneipp H, Kneipp K (2008) SERS–a single-molecule and nanoscale tool for bioanalytics. Chem Soc Rev 37:1052–1060

3. Mungroo NA, Oliveira G, Neethirajan S (2016) SERS based point-of-care detection of food-borne pathogens. Microchim Acta 183:697–707

4. Zhou H, Lin S, Nie Y, et al. (2015) Surface-enhanced resonance Raman scattering (SERRS) simulates PCR for sensitive DNA detection. Analyst 140:7518–7521

5. Pan Y, Guo X, Zhu J, et al. (2015) A new SERS substrate based on silver nanoparticle functionalized polymethacrylate monoliths in a capillary, and it application to the trace determination of pesticides. Microchim Acta 182:1775–1782

6. Ma P, Liang F, Wang D, et al. (2014) Ultrasensitive determination of formaldehyde in environmental waters and food samples after derivatization and using silver nanoparticle assisted SERS. Microchim Acta 182:863–869

7. Bu Y, Lee SW (2015) Flower-like gold nanostructures electrode-posited on indium tin oxide (ITO) glass as a SERS-active substrate for sensing dopamine. Microchim Acta 182:1313–1321

8. Fan M, Andrade GFS, Brolo AG (2011) A review on the fabrication of substrates for surface enhanced Raman spectroscopy and their applications in analytical chemistry. Anal Chim Acta 693:7–25

9. Freeman RG, Grabar KC, Allison KJ, et al. (1995) Self-assembled metal colloid monolayers: an approach to SERS substrates. Science 267:1629–1632

10. Haddada MB, Blanchard J, Casale S, et al. (2013) Optimizing the immobilization of gold nanoparticles on functionalized silicon surfaces: amine- vs thiol-terminated silane. Gold Bull 46:335–341

11. Cintra S, Abdelsalam ME, Bartlett PN, et al. (2006) Sculpted substrates for SERS. Faraday Discuss 132:191–199

12. Min Q, Santos MJL, Girotto EM, et al. (2008) Localized Raman enhancement from a double-hole nanostructure in a metal film. J Phys Chem C 112:15098–15101

13. Hatab NAA, Oran JM, Sepaniak MJ (2008) Surface-enhanced Raman spectroscopy substrates created via electron beam lithography and nanotransfer printing. ACS Nano 2:377–385

14. Polavarapu L, Liz-Marzán LM (2013) Towards low-cost flexible substrates for nanoplasmonic sensing. Phys Chem Chem Phys 15:5288–5300

15. Liu H, Crooks RM (2011) Three-dimensional paper microfluidic devices assembled using the principles of origami. J Am Chem Soc 133:17564–17566

16. Tao H, Chieffo LR, Brenckle MA, et al. (2011) Metamaterials on paper as a sensing platform. Adv Mater 23:3197–3201

17. Ngo YH, Li D, Simon GP, Garnier G (2012) Gold nanoparticle-paper as a three-dimensional surface enhanced Raman scattering substrate. Langmuir 28:8782–8790

18. Zhu Y, Zhang L, Yang L (2015) Designing of the functional paper-based surface-enhanced Raman spectroscopy substrates for colorants detection. Mater Res Bull 63:199–204

19. Zhu Y, Li M, Yu D, Yang L (2014) A novel paper rag as "D-SERS" substrate for detection of pesticide residues at various peels. Talanta 128:117–124

20. Hasi WLJ, Lin X, Lou XT, et al. (2015) Chloride ion-assisted self-assembly of silver nanoparticles on filter paper as SERS substrate. Appl Phys A Mater Sci Process 118:799–807

21. Ngo YH, Li D, Simon GP, Garnier G (2013) Effect of cationic polyacrylamides on the aggregation and SERS performance of gold nanoparticles-treated paper. J Colloid Interface Sci 392:237–246

22. Turkevich J, Stevenson PC, Hillier J (1951) A study of the nucleation and growth processes in the synthesis of colloidal gold. Discuss Faraday Soc 11:55–75

23. Alexander TA, Le DM (2007) Characterization of a commercialized SERS-active substrate and its application to the identification of intact bacillus endospores. Appl Opt 46:3878–3890

24. Ringler M, Schwemer A, Wunderlich M, et al. (2008) Shaping emission spectra of fluorescent molecules with single plasmonic nanoresonators. Phys Rev Lett 100:1–4

25. Xu Y (1995) Electromagnetic scattering by an aggregate of spheres. Appl Opt 34:4573–4588

26. Johnson PB, Christry RW (1972) Optical constants of the Noble metals. Phys Rev B 6:4370–4379

27. Patungwasa W, Hodak JH (2008) pH tunable morphology of the gold nanoparticles produced by citrate reduction. Mater Chem Phys 108:45–54

28. Cañamares MV, Chenal C, Birke RL, Lombardi JR (2008) DFT, SERS, and single-molecule SERS of crystal violet. J Phys Chem C 112:20295–20300

29. Harraz FA, Ismail AA, Bouzid H, et al. (2015) Surface-enhanced Raman scattering (SERS)-active substrates from silver plated-porous silicon for detection of crystal violet. Appl Surf Sci 331:241–247

30. Gardner DJ, Oporto GS, Mills R, Azizi Samir MAS (2008) Adhesion and surface issues in cellulose and nanocellulose. J Adhes Sci Technol 22:545–567

31. Ru EL, Etchegoin PG (2009) Principles of surface enhanced Raman spectroscopy and related plasmonic effects. Elsevier, Amsterdam

32. Deegan RD, Bakajin O, Dupont TF, et al. (1997) Capillary flow as the cause of ring stains from dried liquid drops. Nature 389:827–829

33. Carty DM, Delles C, Dominiczak AF (2008) Novel biomarkers for predicting preeclampsia. Trends Cardiovasc Med 18:186–194

34. Doctor PB, Gokani VN, Kulkarni PK, et al. (2004) Determination of nicotine and cotinine in tobacco harvesters' urine by solid-phase extraction and liquid chromatography. J Chromatogr B 802:323–328

35. Jen JF, Hsiao SL, Liu KH (2002) Simultaneous determination of uric acid and creatinine in urine by an eco-friendly solvent-free high performance liquid chromatographic method. Talanta 58:711–717